A comparison of some kriging interpolation methods for the production of solar radiation maps

Marco Bezzi, Alfonso Vitti

Department of Civil and Environmental Engineering, University of Trento,
via Mesiano 77, 38100 Trento, Italia, tel. +39-0461-882608,
e-mail: alfonso.vitti@ing.unitn.it

Abstract

Many environmental processes depend on the amount of solar radiation at the ground level. Ground measurements are often available, even for long time series, and are used as input for spatial interpolation models to produce continuous maps of solar radiation. The aim of this work is to evaluate the results of different kriging interpolation approaches. This kind of comparison presents a relevant meaning since the availability of a physical model for the direct evaluation of solar radiation, which has been used as reference to validate the interpolation results. The procedure integrates the use of some GIS-GRASS capabilities, such the `r.sun` module which implements the solar radiation physical model, and of the statistical analysis tools provided by the R software package. Some interpolations have been performed taking into account also the values of slope and aspect as geomorphological quantities correlated to the solar radiation value. The study has been performed at different spatial scales to evaluate how resolution affects the results. Accuracy maps have been produced and a brief analysis has been also performed to check the occurrence of significant correlation between geomorphological features and the magnitude of errors. The analyzed solar radiation measurements refer to a zone of the Italian Trentino-Alto Adige region located in the South-East part of the alpine arc.

1. Introduction

Aim of this work is to compare different spatial interpolation techniques, based on the kriging theory, for the estimation of direct solar radiation (DSR) on a geographical domain characterized by a great orographic variability. A physical model for the evaluation of DSR has been applied to produce a reference dataset which served as base to integrate the methods performance analysis. The availability of a reliable DSR values on the entire study area has allowed to extend and to deepen the comparison of the output of the kriging methods being their accuracy estimation based not only on available DSR observed values. This is the main reason why DSR has been chosen as the application filed to test different kriging techniques.

The physical model for the evaluation of DSR at ground level is implemented in the GRASS-GIS module r.sun. This module implements the work of Krcho [8] which defines a physical formulation to compute direct, diffuse and ground reflected solar irradiation for given days and latitude. The model keeps into account the morphological surface features, the atmospheric conditions and the mountains shadowing effects.

In the present work a first dataset, made up of daily records referring to 9 different locations has been used to calibrate the physical model parameters. The data had been measured and collected by the "Ististuto Agrario di San Michele all'Adige" for the period of time 12-21 September 2003 in Trentino, a regional country located in the north-east part of Italy. The observations at ground level have been used to calibrate by the output of the physical model. From the model output map a second dataset has been identified through the extraction of 100 values of DSR randomly distributed over the study area.

Different kriging techniques - simple, ordinary, simple with local mean and kriging with external drift - have been applied to interpolate the 100 values of the second dataset. The choice of using a small number of DSR values has been taken to simulate the typical low availability of DSR measurements. As consequence the experimental semi-variogram has been computed neglecting any directional feature considering the spatial variability as isotropic. Different fitting models have been used to describe the experimental semi-variogram, and to analyze their influence over the interpolation results.

A combination of the morphological features slope and aspect, have been introduced as secondary information in two kriging methods. These information has been derived from the Digital Terrain Model (DTM) of the area using the GRASS-GIS, and have been computed at different spatial resolutions to estimate if and how the spatial scale affects the results. All the statistical analyses have been performed using the R statistical software and the `gstat` package.

The performance of the interpolators has been assessed and compared in terms of the root mean square errors (RMSE) obtained from the difference between the predicted values and the first dataset information, i.e. measured values. Error maps for the entire domain have been produced comparing the kriging results to the DSR map produced by the GRASS-GIS module `r.sun`. Moreover, some statistical features of such errors maps has been analyzed to classify the kriging methods performance and to evaluate the reliability of the predicted DSR values over an orographically complex domain.

2. Materials and Methods

The study area is 80 km x 20 km and it is located in the Trentino region, in the north-east part of the Italy. It is characterized by a great variation of the landscape geomorphological features and is mainly interested by a big valley, in the middle, (mean altitude 200 m) and by mountains elsewhere (mean altitude 2000 m). The zone has been chosen for the availability of solar radiation records provided by 9 meteorological stations managed by the "Istituto Agrario di San Michele all'Adige, Trento - Italy".

The observation period, 12-18 September 2003, has been chosen because of the high-pressure and clear sky conditions during the entire week. The direct solar radiation values have been used to calibrate the parameters of the module `r.sun`. The more difficult step, in the calibration of the model, has been the choice of the atmospheric turbidity coefficient. A correct estimation of such coefficient has been facilitate by the good and spatially uniform atmospheric conditions. The best accordance between measured values and the r.sun output has been obtained setting the Linke turbidity coefficient equal to 2.0; for more details on the Linke coefficient see the manual page of the r.sun module. The biggest difference obtained between the r.sun output and the measured values has been less than 4.3%.

The `r.sun` output map has therefore been considered as reference for the further analyses. A number of 100 values, randomly distributed over the study area, have been extracted from this map and used as input dataset for the kriging interpolations. Figure 1 shows the location of the 9 meteorological stations (in red) and of the 100 new locations extracted from the r.sun output map (in yellow).

Table 1 indicates the comparison between the solar radiation values recorded at the 9 meteorological stations and the values estimated using the module `r.sun`. Each difference is less than 5% supporting the choice of using radiation values derived from the `r.sun` output as input for the kriging methods.

	1 *San Michele*	*2* *Trento sud*	*3* *Rovereto*	*4* *Vigolo Vattaro*	*5* *Faedo*	*6* *Cles*	*7* *Cavedine*	*8* *Fondo*	*9* *Malga Flavona*
`r.sun`	5170	5330	5197	5001	5653	5258	5058	5505	4642
measure	5022	5264	4892	4896	5839	5084	5171	5366	4936

Table 1: direct solar radiation values from the `r.sun` output and measured values.

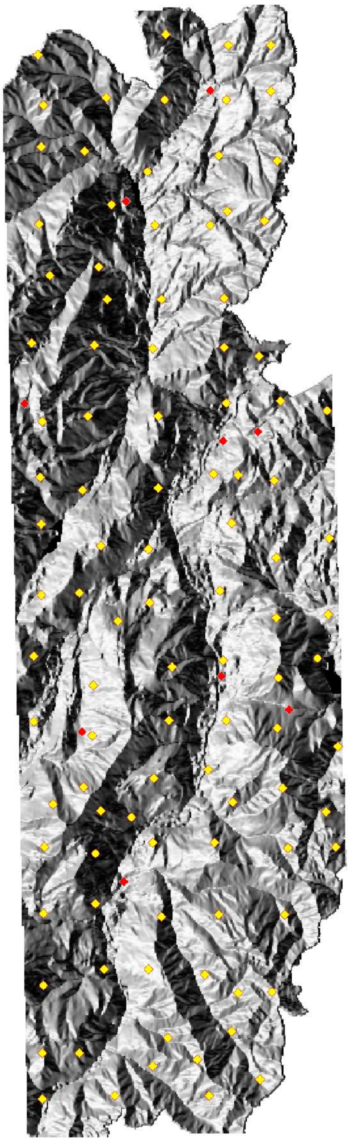

Figure 1: location of the 9 meteorological stations (red) and of the 100 locations extracted from the `r.sun` output map (yellow).

3. Procedure

In this section a schematic description on the data preparation and on the steps followed to perform the comparison are reported. It is also described how the landscape morphological features have been treated to produce the secondary information for the kriging methods that keep into account secondary data. Some discussions on the accuracy of the kriging outputs and on the influence of the semi-variogram fitting model on the results follow. In Figure 2 it is reported a schema of the relations defined in developing the comparison procedure.

Individuation of the period of time

The studied period has been chosen for the condition of clear sky immediately following two raining days. For this period, 12-18 September 2003, daily data of DSR have been extracted from the database of the "Istituto Agrario di San Michele all'Adige", for each of the 9 meteorological stations considered. The DSR weekly mean value for each station has therefore been computed.

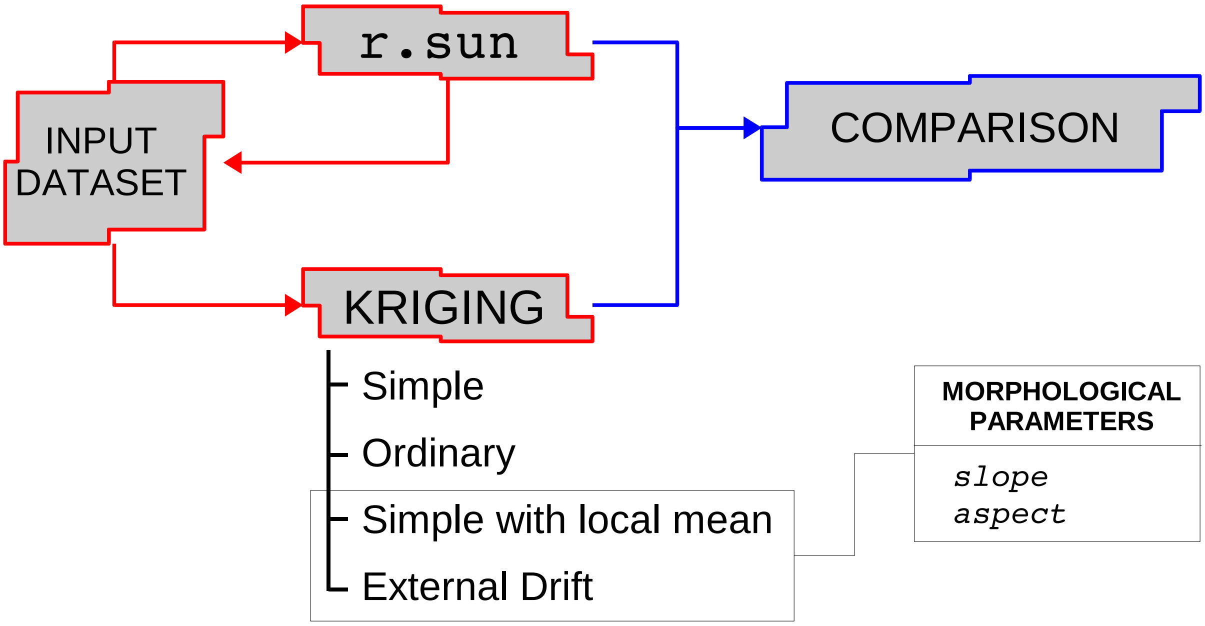

Figure 2: procedure schema.

<u>*Develop of Slope and Aspect maps and reclassification*</u>

Based on the 10mx10m spatial resolution DTM provided by the “Provincia Autonoma di Trento” (local government agency), slope and aspect maps have been developed at the spatial resolution of: 100m, 500m and 1000m. The information about slope and aspect, angles in degrees, have been re-classified by means of discrete intervals to assign each cell (pixel) a single value of class. Tables 2 and 3 report the classifications adopted, while Table 4 reports the combined re-classification of the slope and aspect classes which has been used to define the morphological index.

class	*1*	*2*	*3*	*4*	*5*	*6*
values [°]	0 -- 5	5 -- 10	10 -- 20	20 – 30	30 -- 40	40 -- 90

Table 2: slope values re-classification.

class	*10 East*	*20 N-E*	*30 North*	*40 N-W*	*50 West*	*60 S-W*	*70 South*	*80 S-E*
values [°]	-22.5 - 22.5	22.5 - 67.5	67.5 - 112.5	112.5 - 157.5	157.5 – 202.5	202.5 – 247.5	247.5 – 292.5	292.5 – 337.5

Table 3: aspect values re-classification.

The classes of slope and aspect have been therefore combined together to obtain 48 classes used as morphological index to be correlated to the values of DSR.

Figure 3 reports the map of the 48 combinations of slope and aspect classes for the study area. This slope and aspect combined classification has been used to develop a linear model describing the DSR as a function of this morphological index. This information has been used as secondary data. The estimated linear model has been used to over-impose, to the simple kriging method, a local mean estimator. The relation between DSR and the defined morphological index has also allowed to over-impose an external drift to the kriging estimator.

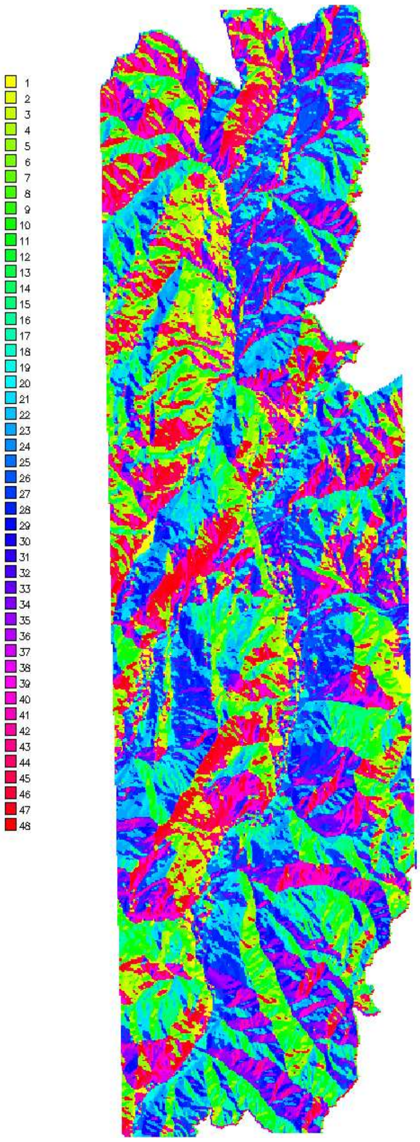

Figure 3: map of the reclassified values of slope and aspect.

Choice of the Linke turbidity coefficient

Different values of the Linke turbidity coefficient have been tested in the `r.sun` applications. The estimation of the best parameter value for the study area has been performed comparing the `r.sun` output with the measured values of DSR at the 9 meteorological stations. The best agreement has been obtained setting the Linke turbidity coefficient to the value of 2.0.

	Aspect classes							
Slope classes	*10*	*20*	*30*	*40*	*50*	*60*	*70*	*80*
1	11	21	31	41	51	61	71	81
2	12	22	32	42	52	62	72	82
3	13	23	33	43	53	63	73	83
4	14	24	34	44	54	64	74	84
5	15	25	35	45	55	65	75	85
6	16	26	36	46	56	66	76	86

Table 4: slope and aspect combined re-classification: morphological index.

Extraction of the 100 values for the interpolation procedure

The physical model has been applied to the study area and a DSR value has been generated for each single cell of the grid describing the study area. The values of DSR have been estimated for each day between the 12 and 18 September 2003. The mean daily values have been therefore calculated and used as input data for the interpolation procedure. For each location the value of the slope and aspect combined classification has also been extracted. In Figure 4 the `r.sun` output map is reported.

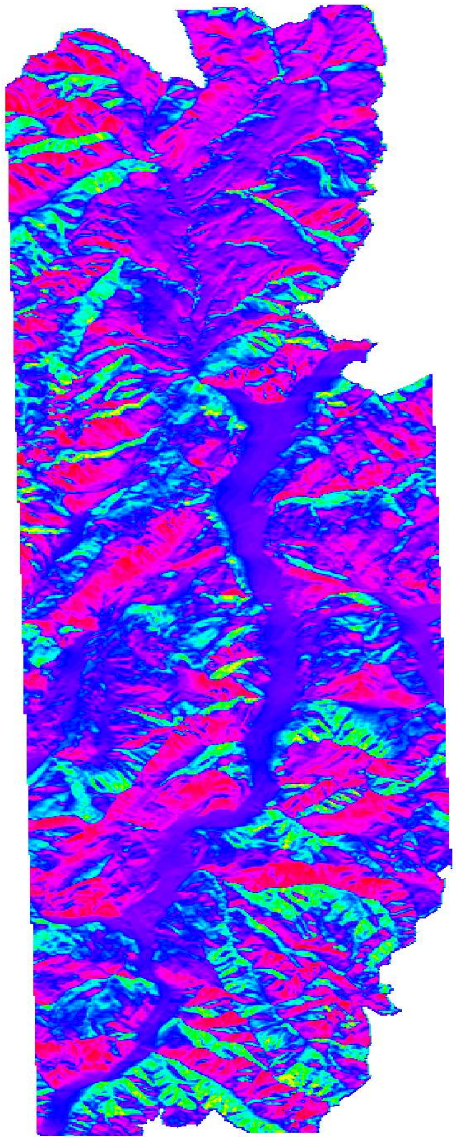

Figure 4:direct solar radiation map obtained from the GRASS module `r.sun`*.*

For the data interpolation different kriging techniques have been applied. Kriging is a stochastic technique similar to inverse distance weighted averaging where a linear combination of weights at known points is used to predict the value at unknown points. The kriging system is expressed in terms of covariances which are commonly derived by the estimation and the modeling of a semi-variogram: a measure of spatial correlation between two points. The following kriging approach have been used:

- simple kriging;
- ordinary kriging;
- simple kriging with local mean;
- kriging with external drift.

The kriging interpolation has been computed by linking GRASS to the R statistical environment and by the use of the R spatial package `gstat`.

Derivation of the experimental semi-variogram and choice of the fitting models

All the 100 values composing the second dataset have been used to derive the experimental semi-variogram. No directional variability has been taken into account in the derivation of the semi-variogram. The models chosen to fit the experimental semi-variograms are the exponential, the spherical and the gaussian model. All these three models have been used for each kriging methods. The differences between the predicted values and the measured values, at the 9 locations composing the first dataset, as been compared to describe the influence on the results of the semi-variogram fitting model adopted. Figure 5 shows the derived experimental semi-variogram and the three fitting models.

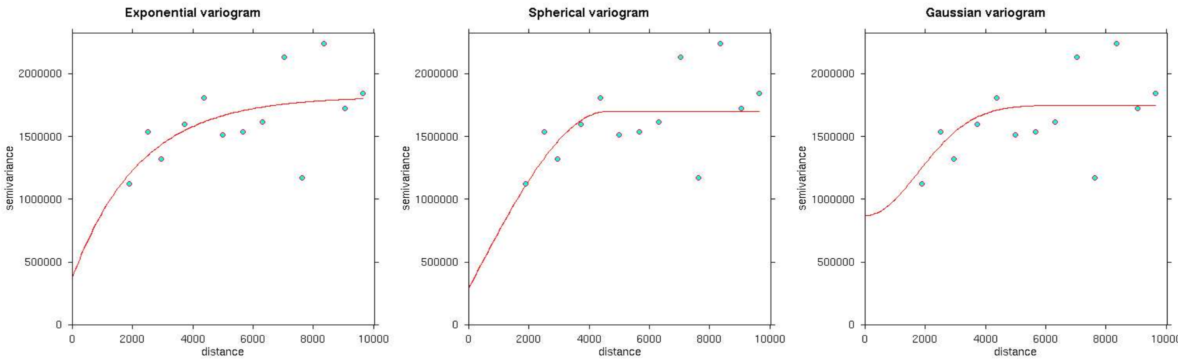

Figure 5: experimental semi-variogram of direct solar radiation and fitting models.

Simple and Ordinary Kriging

The application of the simple kriging technique requires the stationarity mean value of the quantity to be predicted to be know. In this work, since the objective was not a pure application of kriging but the comparison of different methods and being a reliable physical model available, the mean value of DSR has been computed from the `r.sun` output. The ordinary kriging does not require the mean to be known, being it evaluated from the input data.

Accounting for spatial resolution

The physical model implemented in the `r.sun` module has been applied at three different spatial resolutions. The original 10x10 m DTM has been re-sampled to obtain DTMs at the resolutions of 500x500m and 1000x1000m. From the three DTMs the slope and aspect maps have been developed and re-classified according to the slope and aspect combined reclassification rules. For each spatial resolution the map of the `r.sun` DSR values and the map of the morphological index have therefore been developed. The value of the morphological index has also been extracted for all the 9 locations were measurements were available. At a given station the three values of the morphological index differed since they have been derived from DTMs at different spatial resolution.

Estimation of the relation between DSR and slope and aspect combined classification

To improve the prediction performance two kriging methods that allowed soft data accounting have been applied, in particular the simple kriging with local means and kriging with an external drift have been applied. The secondary information have been extracted from each DTMs, since the value of DSR varies as a function of the orientation of the surface, i.e. at a given time, on the angle between the solar beams and the surface. To model this dependence the slope and aspect angles have been combined to define a morphological index that has been chosen as secondary data for the two kriging methods.

The mean value of the DSR has been evaluated for each class of the slope and aspect combined reclassification, i.e. for each morphological index. The DSR mean values have therefore been arranged in increasing order and labeled with their position index. The same labels have been used to update the value of the morphological index obtaining a proportional relation between the DSR mean values and the morphological index. A fitting linear model has been estimated to analytically describe such relation.

To evaluate how the spatial resolution influence the kriging prediction three linear models have been estimated, one for each spatial resolution. The models describe the relation between the DSR values obtained from the `r.sun` maps and the morphological index for the 100 locations used as input for the kriging methods. Both the `r.sun` DSR values and the morphological index depend on the DTM resolution which, as consequence, affects also the regression coefficients of the linear model.

Figure 6 shows the variability of the DSR values for each morphological index for the study area, the box-plots are derived by the `r.sun` map at the 100x100m spatial resolution.

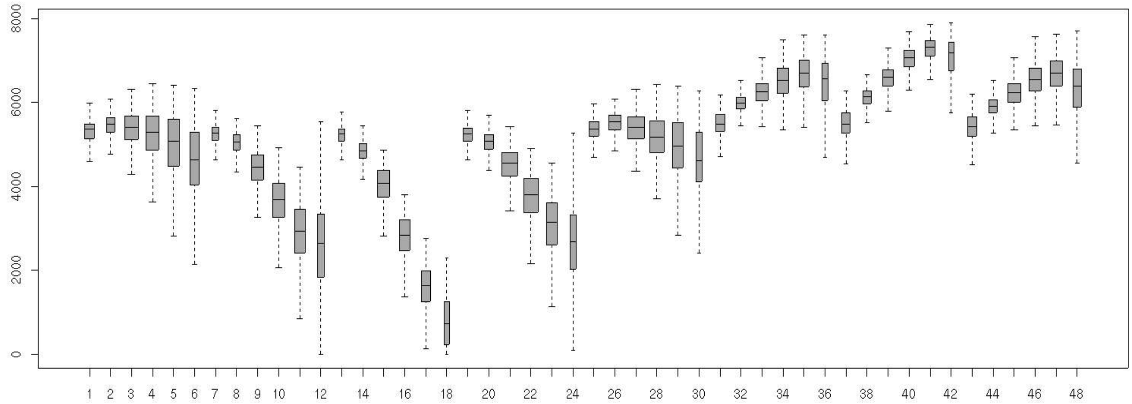

Figure 6: variability of the direct solar radiation values for each morphological index.

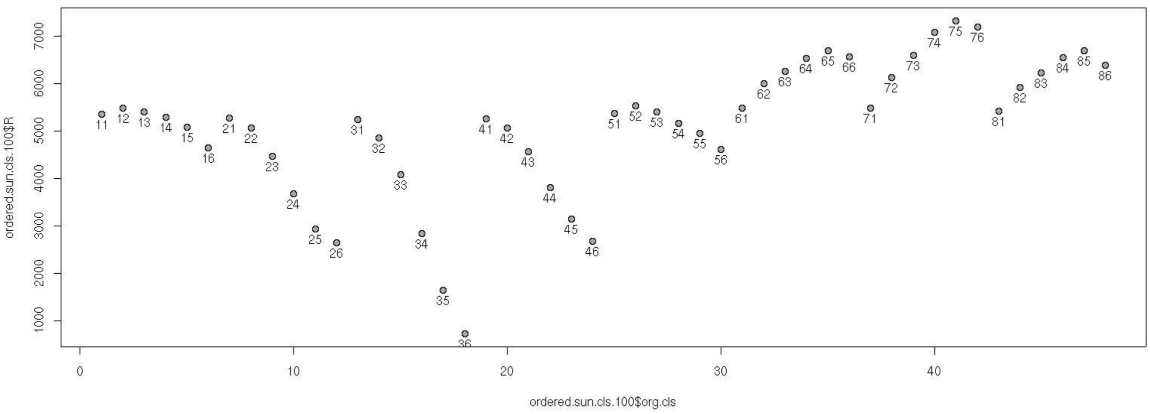

Figure 7: means of the direct solar radiation values for each morphological index.

Figure 7 reports only the DSR mean values for each morphological index. Under each point it is reported the class value of the slope and aspect combined reclassification. Eight main groups can be individuated on the plot, each group refer to one of the eight aspect classes defined in Table 3. Within each group, the six points refer to the slope classes defined in Table 2. It can be noted that the firsts five groups present a similar behavior: greater values of the slope angle correspond to a lower value of the mean DSR. The last three groups refer to surfaces oriented toward South, South-East and South-West where at increasing values of the slope angle correspond greater values of the DSR. Figure 8 shows the DSR means arranged in increasing order and the fitting linear model. Under each point it is reported the original class value of the slope and aspect combined reclassification, while the position index is reported over the points defining the new value of the morphological index. Table 5 reports the regression coefficients of the estimated linear models.

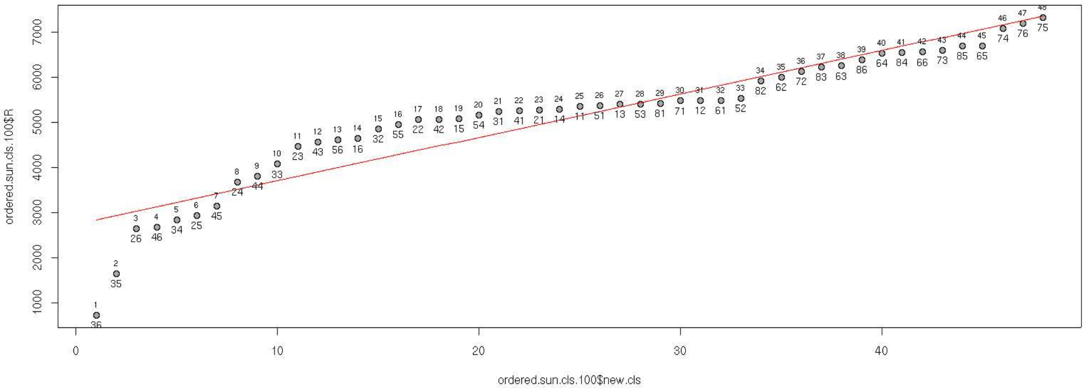

Figure 8: means of the direct solar radiation values arranged in increasing order and linear model.

DSR=a+b (morph. index)		a	b
entire map	100x100 m	2747	96
100 pts	100x100 m	3435	102
100 pts	500x500 m	2522	148
100 pts	1000x1000 m	3620	98

Table 5: regression coefficients of the estimated linear models.

The firsts two values have been obtained considering the `r.sun` map and the morphological indexes derived from the 100x100m DTM, i.e. they have been estimated considering an huge number of points. The other values have been obtained considering the 100 points used as input for the kriging interpolations and refer to the spatial resolution of 100x100m, 500x500m and 1000x1000m. Using only the 100 points to derive the linear model all the possible values of the morphological index may not be included in the regression analysis. In fact, if a particular value of the morphological index can not be renamed, according to the position index of its DSR value, that value can not be included in the derivation of the linear model. Therefore, during the kriging application, when the linear model is used to estimate the value of the local DSR mean, a wrong value is evaluated for the morphological index not used to derive the model.

Application of Simple Kriging with Local Means and Kriging with an External Drift

Simple kriging with local means and kriging with an external drift use the secondary information to derive the local mean of the primary quantity, then the kriging system is solved on the corresponding residuals. The regression coefficients are derived once and independently from the kriging system for the SKLM approach, whereas, in the KED approach, the trend coefficients are implicitly estimated through the kriging system. For each of the three fitting models adopted the two techniques have been applied at the three spatial resolution, i.e. different regression coefficients have been used to describe the relation between the DSR and the morphological index.

4. Results

Simple and Ordinary Kriging

The output of the two models can not be considered of any usefulness or usability. The DSR predicted maps do not present any similarity with the output of the physical model. The predicted values can be compared to the `r.sun` values in terms of magnitude, their are “numerically correct” but they do not describe, in any way, the spatial variability of the interpolated quantity. The outputs are similar to the one obtainable by the application of an inverse distance weighted algorithm. The only possibility to improve the output of these to kriging methods is to use a greater number of points where

DSR is known.

Figure 9 shows the DSR maps obtained and the `r.sun` output map. The spatial resolution do not affects the results: changing the grid resolution only lead to a geometrically more detailed map where the predicted values do not improve their capabilities to describe the behavior of the interpolated quantity.

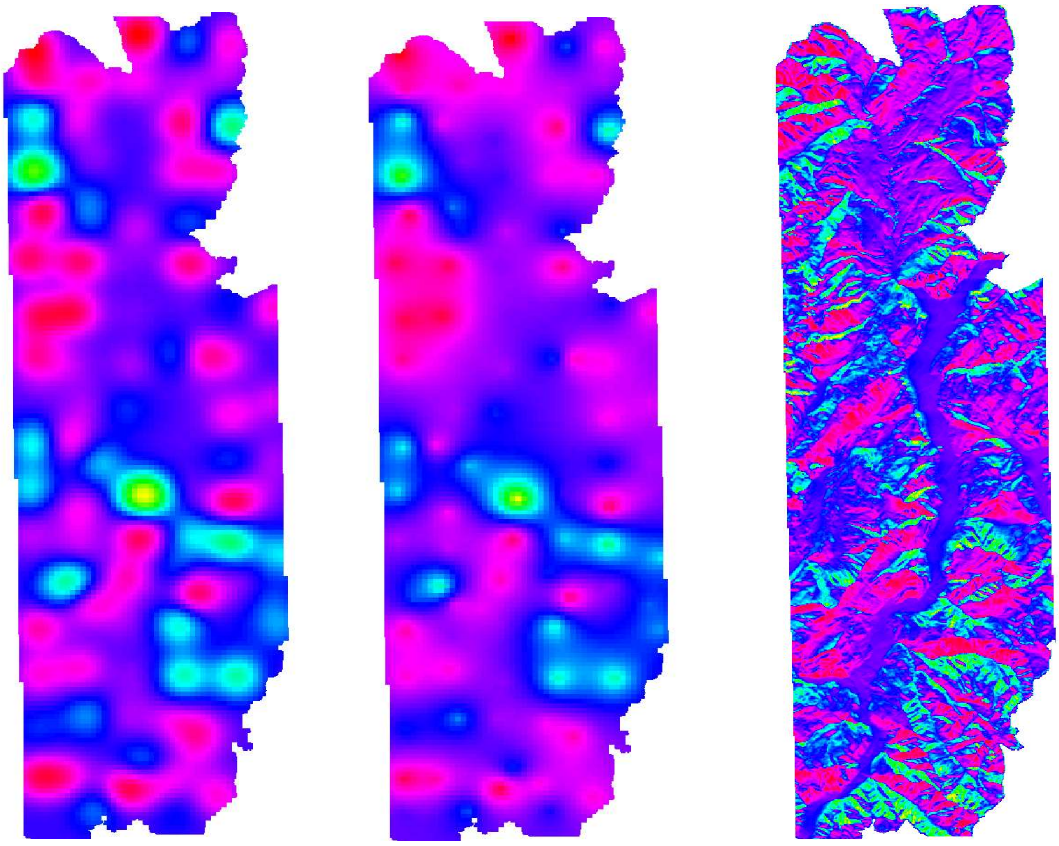

Figure 9: direct solar radiation map with simple kriging, ordinary kriging and `r.sun` outputs.

Tables 6 and 7 report the differences between the kriging predicted values and the DSR values measured at the 9 meteorological stations, RMSE are also reported. For both the methods the results obtained fitting the experimental semi-variogram with the Gaussian model are the closer to the measured values. Using the Spherical model do not differ to much from the use of the Gaussian, while the Experimental model leads to the biggest differences between predicted and observed values.

Stations	*DSR*	*SK 500 Exp*	*diff*	*SK 500 Sph*	*diff*	*SK 500 Gau*	*diff*
Trento sud	5264.68	4835.28	429.41	5050.73	-215.45	5015.89	-215.45
San Michele	5022.22	5283.89	-261.67	5176.91	106.98	5184.23	106.98
Rovereto	4892.46	5488.34	-595.88	5342.28	146.06	5330.15	146.06
Vigolo Vattaro	4896.43	4531.92	364.51	4479.79	52.12	4603.85	52.12
Faedo	5839.29	5336.29	503.00	5175.26	161.02	5191.51	161.02
Cles	5083.73	5286.01	-202.28	5311.16	-25.15	5269.24	-25.15
Cavedine	5171.03	5569.34	-398.31	5646.58	-77.24	5508.09	-77.24
Fondo	5366.27	5524.01	-157.74	5377.67	146.34	5339.41	146.34
Malga Flavona	4936.11	5908.34	-972.23	5674.71	233.63	5594.59	233.63
RMSE		490.29		435.9		389.77	

Table 6: differences between simple kriging predicted values and measured values of direct solar radiation.

Stations	DSR	OK 500 Exp	diff	OK 500 Sph	diff	OK 500 Gau	diff
Trento sud	5264.68	4911.69	353	5166.44	-254.75	5149.99	16.45
San Michele	5022.22	5380.26	-358.04	5334.51	45.76	5349.97	-15.46
Rovereto	4892.46	5588.42	-695.96	5519.74	68.68	5508.7	11.04
Vigolo Vattaro	4896.43	4615.13	281.3	4588.3	26.83	4736.55	-148.25
Faedo	5839.29	5441.88	397.41	5367.64	74.24	5379.23	-11.59
Cles	5083.73	5351.89	-268.16268.16	5372.93	-21.03	5370.17	2.76
Cavedine	5171.03	5631.86	-460.82	5726.84	-94.98	5625.78	101.06
Fondo	5366.27	5606.11	-239.84	5504.79	101.32	5481.93	22.86
Malga Flavona	4936.11	6052.54	-1116.42	5850.81	201.72	5782.34	68.47
RMSE		533.59		479.17		441.7	

Table 7: differences between ordinary kriging predicted values and measured values of direct solar radiation.

<u>*Simple Kriging with Local Means and Kriging with an External Drift*</u>

The resulting maps of the two methods are closer to the `r.sun` output map than the maps obtained applying the previous kriging techniques. The introduction of a secondary information improve the kriging capability to describe the spatial variability of DSR. The use of the morphological index allow the SKLM and the KED to predict DSR values with a more reliable “physical meaning”.

Table 8 reports the values of the DSR measured at the 9 meteorological stations and the SKLM predicted values for the three models used to fit the experimental semi-variogram and for the three spatial resolutions. Table 9 reports the same information for the KED.

Stations	DSR	SKLM 100 Exp	diff	SKLM 100 Sph	diff	SKLM 100 Gau	diff
Trento sud	5264.68	5557.82	-293.14	5745.28	-187.46	5661.38	83.9
San Michele	5022.22	5728.57	-706.34	5699.88	28.68	5687.31	12.57
Rovereto	4892.46	6958.62	-2066.16	6940.04	18.58	6957.81	-17.76
Vigolo Vattaro	4896.43	5070.97	-174.54	4973.05	97.92	5047.26	-74.21
Faedo	5839.29	4790.50	1048.79	4781.70	8.80	4805.69	-23.99
Cles	5083.73	5244.26	-160.53	5299.81	-55.54	5208.62	91.19
Cavedine	5171.03	5635.73	-464.70	5523.18	112.56	5638.78	-115.61
Fondo	5366.27	6222.79	-856.52	6106.91	115.87	6165.00	-58.09
Malga Flavona	4936.11	5284.35	-348.24	5251.87	32.48	5248.50	3.37
RMSE		887.00		870.89		877.27	

Table 8: differences between simple kriging with local mean predicted values and measured values of direct solar radiation.

Stations	DSR	UK 100 Exp	diff	UK 100 Sph	diff	UK 100 Gau	diff
Trento sud	5264.68	5548.78	-284.10	5763.51	-214.73	5729.54	33.97
San Michele	5022.22	5936.67	-914.45	5907.10	29.57	5899.80	7.30
Rovereto	4892.46	5099.98	-207.52	5120.32	-20.34	5124.22	-3.90
Vigolo Vattaro	4896.43	4369.19	527.23	4286.64	82.56	4366.70	-80.07
Faedo	5839.29	5465.14	374.15	5463.53	1.61	5472.37	-8.84
Cles	5083.73	5462.88	-379.15	5488.59	-25.71	5464.75	23.84
Cavedine	5171.03	4608.68	562.35	4586.99	21.69	4652.80	-65.81
Fondo	5366.27	6005.78	-639.51	5877.69	128.09	5914.11	-36.42
Malga Flavona	4936.11	5341.50	-405.39	5158.15	183.35	5079.27	78.88
RMSE		517.61		517.76		493.24	

Table 9: differences between kriging with external drift predicted values and measured values of direct solar radiation.

Fitting the experimental semi-variogram with the Gaussian model produces, for both the methods, the smaller differences between predicted and measured values. Using the Spherical model leads to similar results, only for the SKLM, performed at the 100x100m spatial resolution, the RMSE are less than the Gaussian RMSE. The Exponential model, for all the spatial resolutions, presents the biggest errors.

The performance comparison of these two methods has also been performed in terms of the difference between the DSR predicted values and the DSR obtained by the application of the physical model implemented in the GRASS module `r.sun`. Figures 10 and 11 report, for the SKLM and for the KED methods respectively, the the `r.sun` output map, the kriging resulting maps and their differences, all the maps refer to the 500x500m spatial resolution.

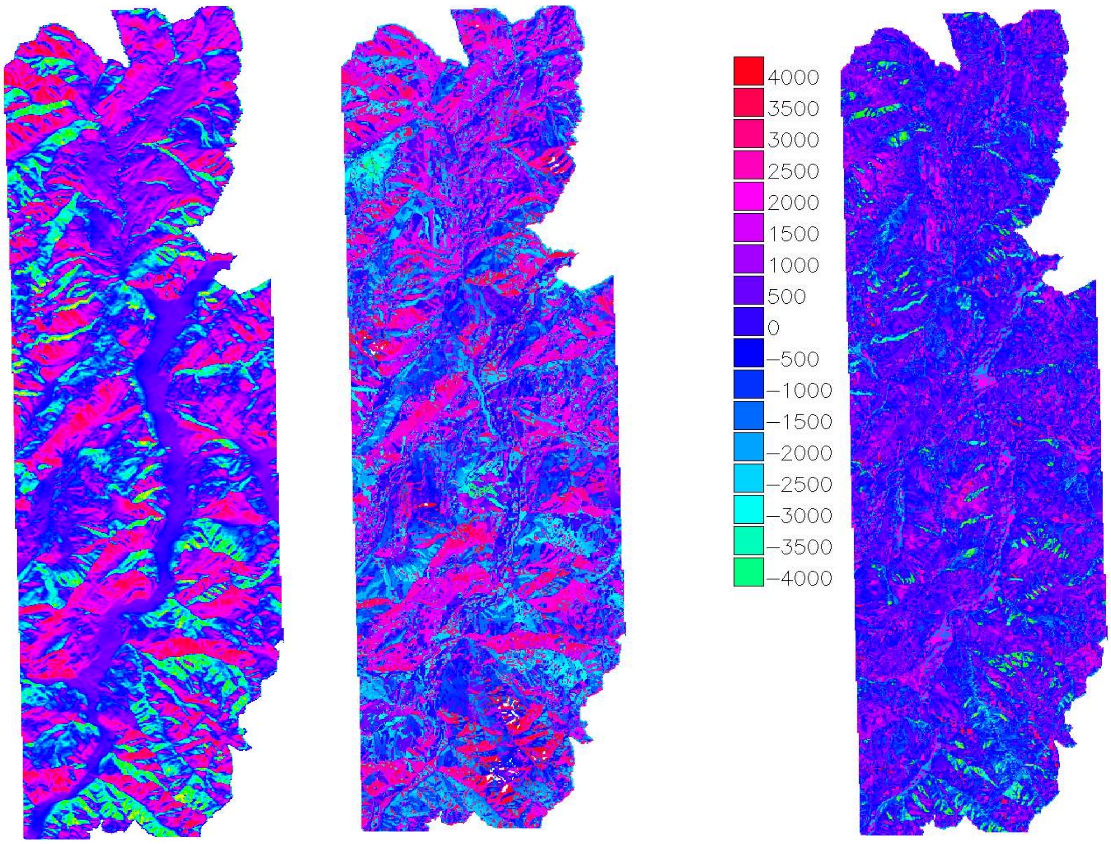

Figure 10: `r.sun` *output map, simple kriging with local mean (100x100 m) map and differences map.*

The main statistical properties of the errors are reported in table 10 for the SKLM, in table 11 for the KED. For the SKLM, the smaller mean errors are obtained performing the analysis at the 1000x1000m resolution and using the Experimental model to fit the experimental semi-variogram. For the KED the smaller mean errors are obtained at the 500x500m spatial resolution, using the Gaussian model. Performing the prediction at the 100x100m spatial resolution, for both the methods leads to greater, but still acceptable, mean errors.

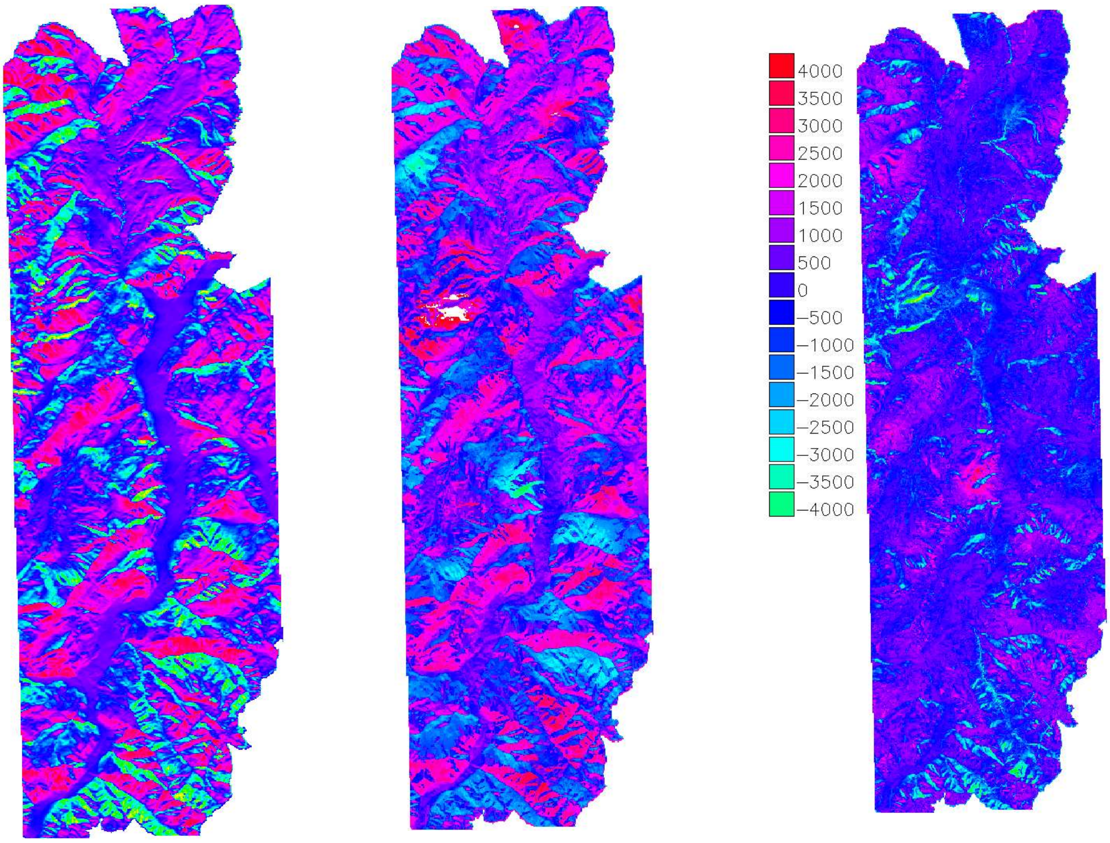

Figure 11: `r.sun` *output map, kriging with external drift map (100x100 m) and differences map.*

	100						500						1000					
	Min	**1stQ**	**Med**	**Mean**	**3rdQ**	**Max**	**Min**	**1stQ**	**Med**	**Mean**	**3rdQ**	**Max**	**Min**	**1stQ**	**Med**	**Mean**	**3rdQ**	**Max**
Exp	-7862	-605.60	-15.77	-71.63	551.40	4260	-3381	-237.7	213.8	455.7	839.4	5461	-7596	-627.9	80.45	-24.82	743.1	4352
Gau	-7621	-586.40	-13.01	-67.49	539.70	4238	-3378.	-257.4	223.4	463.1	838.2	5462	-7206	-646.9	68.32	-43.64	698.7	4276
Sph	-7900	-605.80	-15.18	-69.18	553.90	4531	-3374	-261.4	220.1	460.8	845.1	5562	-7330	-656.9	73.66	-36.74	710.1	4511

Table 10: main statistical properties of the .errors of the simple kriging with local mean output.

	100						500						1000					
	Min	**1stQ**	**Med**	**Mean**	**3rdQ**	**Max**	**Min**	**1stQ**	**Med**	**Mean**	**3rdQ**	**Max**	**Min**	**1stQ**	**Med**	**Mean**	**3rdQ**	**Max**
Exp	-6418	-537.7	-115.6	-217.5	259.4	3434	-3609	-293.1	73.95	31.24	430.3	2743	-5058	-558.1	-30.16	-169.2	413.4	3981
Gau	-5795	-547.8	-121.4	-219.8	234.5	2978	-3601	-295.1	69.16	27.06	423.8	2575	-4741	-527.2	-22.0	-169.3	378.0	3561
Sph	-6500	-577.4	-124.8	-221.2	251.8	3669	-3737	-305.0	64.69	27.23	434.8	2905	-4938	-530.1	-29.34	-167.1	397.1	4320

Table 11: main statistical properties of the .errors of the kriging with external drift output.

Figure 12 describes the distribution of the errors obtained applying the KED method at the 500x500m spatial resolution with the Gaussian fitting model.

The spatial distribution of the differences between predicted and physical DSR values have also been analyzed. The errors distribution, within each class of the slope and aspect combined reclassification, i.e. for the morphological index, has been computed to check whether biggest or smaller errors belong to some specific class.

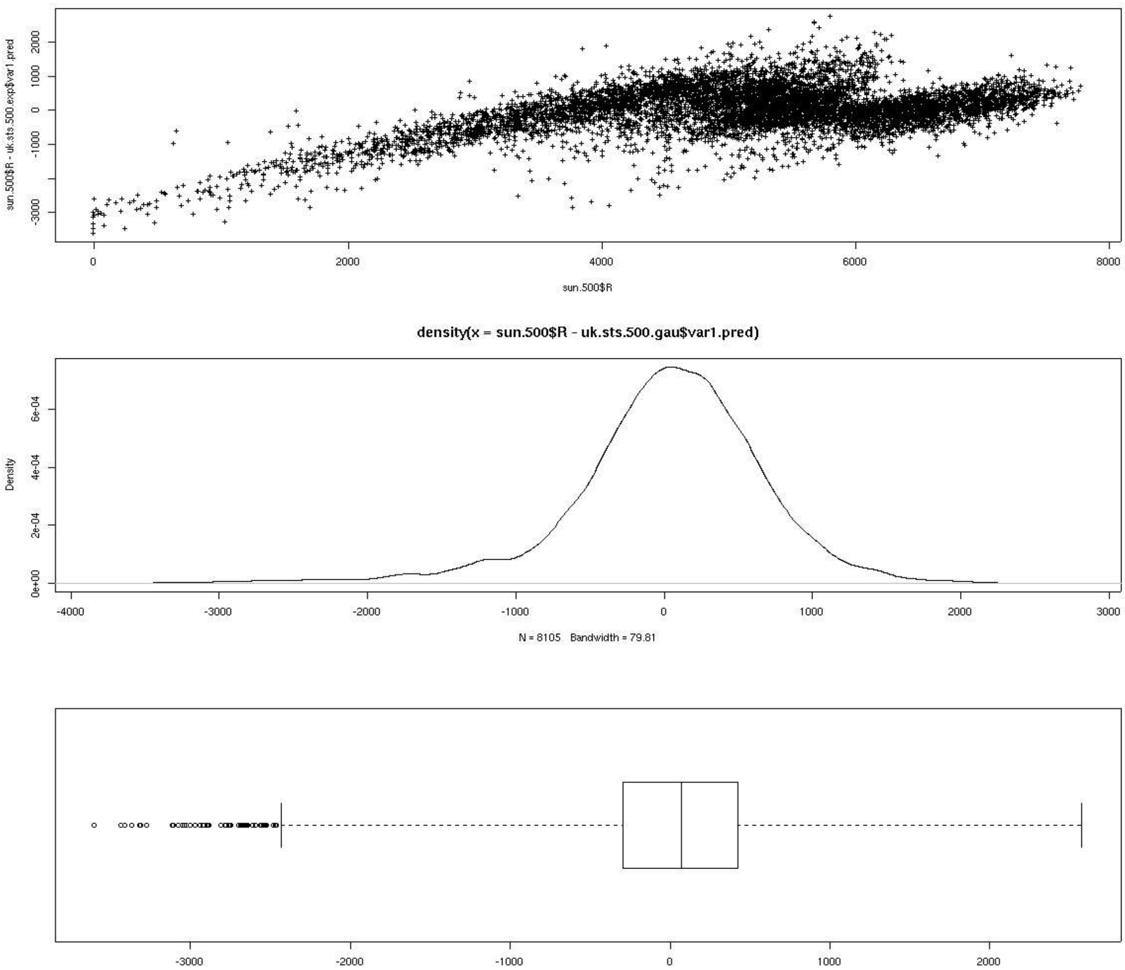

Figure 12: errors distribution of the kriging with external drift output, 500x500 m spatial resolution, Gaussian fitting model.

Figure 13 reports errors over morphological index box-plots for the SKLM at the three spatial resolutions, the predictions have been performed using the Exponential model. At each resolutions some outliers can be easily identified. The source of these big differences, between predicted and physical DSR values, has to be lead back to the linear model used to describe the relation between DSR and morphological index. In fact, the classes where the the biggest errors appear were the classes not presented in the 100 values dataset used to derive the model. The values of these classes differ in the plots since the morphological indexes have been derived from DTMs at different spatial resolutions, the 100 points belong to different classes depending on the original DTM resolution. The same analysis has been performed for the KED errors.

Figure 14 reports errors over morphological index box-plots obtained when the Gaussian model is used to fit the experimental variogram. The errors distribution present a lower variability with respect to the SKLM errors distribution. For the KED application, in fact, the applied linear model has been derived using the `r.sun` output map and the morphological index map at the 500x500m resolution, i.e. all the morphological indexes were available for the regression analysis. The errors within the first classes are greater that the others which have a mean value closer to zero. This behavior can still be lead back to the features of the linear model used to describe the relation between primary and secondary information.

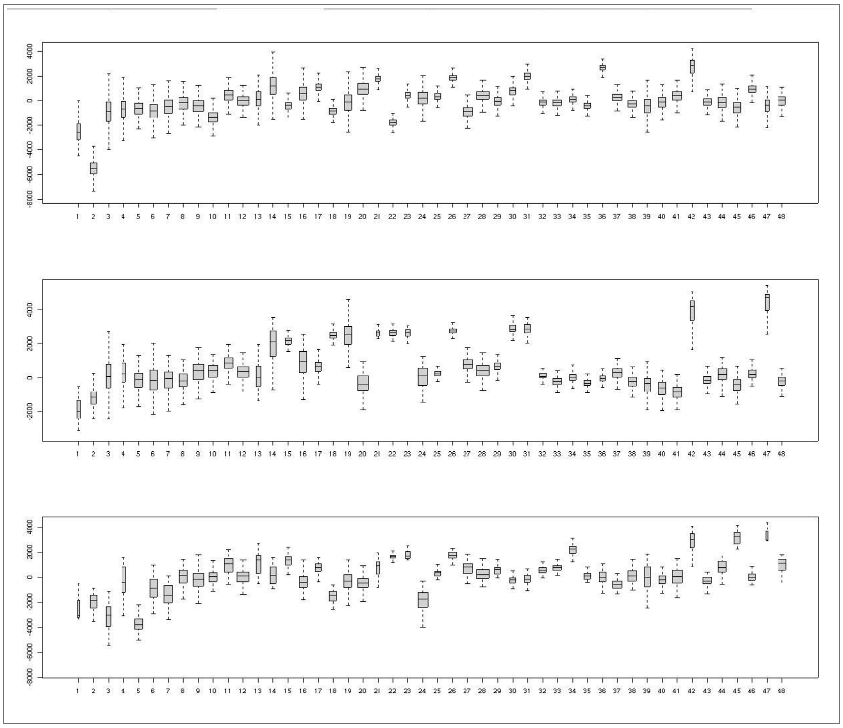

Figure 13: errors versus morphological index box-plots for the simple kriging with local mean, 100x100, 500x500 and 1000x1000 m spatial resolutions, Exponential fitting model.

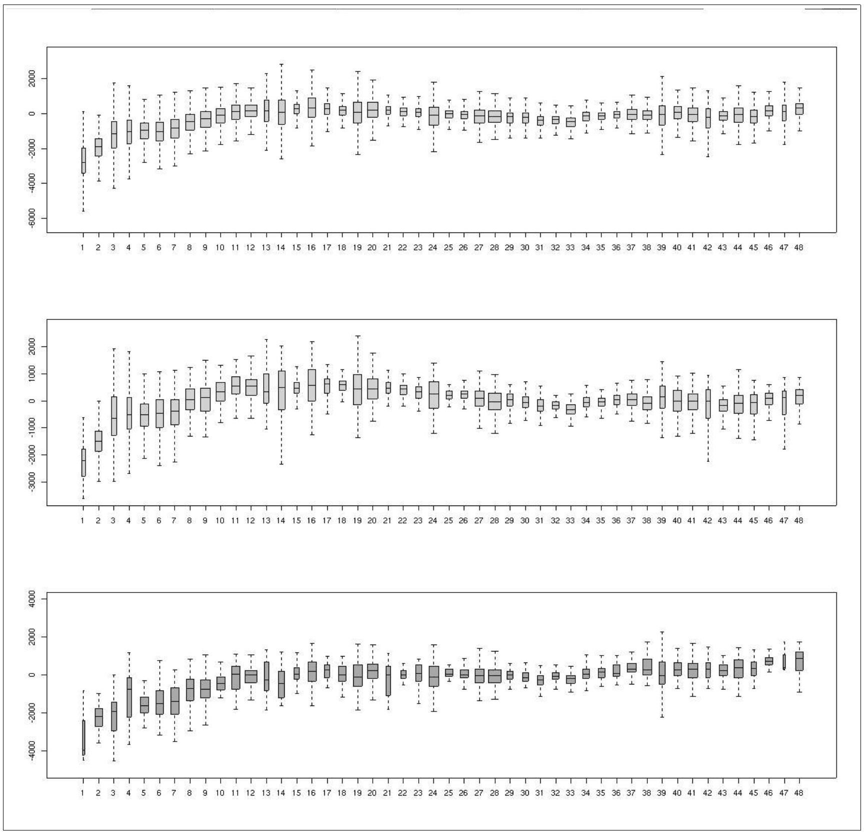

Figure 14: errors versus morphological index box-plots for the kriging with external drift, 100x100, 500x500 and 1000x1000 m spatial resolutions, Gaussian fitting model.

5. Conclusions

Four spatial interpolation methods, based on the kriging technique, have been applied for the derivation of direct solar radiation maps. The predicted values have been compared to observed values at 9 ground control points. The available measurements have been used to calibrate a physical model, implemented in the GRASS-GIS `r.sun` module, to derive a reliable direct solar radiation map for the entire study area. This map served as reference to evaluate the accuracy of the kriging output maps and to evaluate the capability of the kriging methods to describe the spatial variability of DSR.

The results obtained by the application of the Simple and Ordinary kriging do not provide a satisfactory representation of the spatial variability of the DSR. A better agreement with the physical model has been obtained providing secondary information for the application of Simple kriging with local means and kriging with an external drift methods. As secondary information a morphological index has been derived by the digital terrain model combining the terrain slope and aspect values. A linear model has been derived to describe the relation between DSR and this morphological index. The model has been used to estimate the local mean for the SKLM application and as external drift for the KED application.

The experimental semi-variogram has been fitted using the Exponential, the Spherical and the Gaussian models to evaluate their influence on the kriging results. The performance of the four models has been assessed at three different spatial resolutions, 100x100m, 500x500m and 1000x1000m, by comparing the differences between predicted values and measurements. A further analysis has been performed comparing the predicted maps with the output of the physical model.

Considering the root mean square errors obtained from the available measurements the best results have been obtained, for all the methods, using the Gaussian model to fit the experimental semi-variogram. The best agreement between predicted and physical values have been obtained using the Gaussian method for the KED and the Exponential for the SKLM. The spatial resolution influence the estimation of the linear model coefficients but relevant differences can not be observed in the resulting DSR maps. No particular correlation has been found between the errors distribution and the terrain morphological features considered by means of the definition of a slope and aspect combined reclassification.

The comparison presents a significant meaning because of the morphological complexity of the domain, where the spatial variability of the studied quantity can not be described only by a function of the space. The secondary information introduced have leaded to “numerically” corrected results that respect the “physical behavior” of the direct solar radiation. This underlines the importance of the secondary data for the correct prediction of the spatial distribution of the studied quantity.

The study has been performed integrating the functionalities of the GRASS-GIS and of the R statistical package. This has allowed the correct management of the geographical information and the possibility to use geo-statistical tools to analyze the data.

6. References

[1] Bailey T., Gatrell A. Interactive spatial data analysis. Harlow: Longman, 1995.
[2] Bedient P.B., Huber W.C.Hydrology and Flooplain Analysis: Second Edition, Addison-Wesley, New York - NY, 1992.
[3] Bivand R.S. Using the R statistical data analysis language on GRASS 5.0 GIS database files. Computers &Geosciences, 26, p. 1043-1052, 1999.
[4] Bivand R., Neteler M. Open Source geocomputation: using the R data analysis language integrated with GRASS GIS and PostgreSQL data base systems. GeoComputation, 2000.
[5] Edzer J., Pebesma and Cees G. Wesseling Gstat: a program for geostatistical modelling, prediction and simulation. Computers & Geosciences Vol. 24, No. 1, pp. 17-31 (a paper full with typos), 1998.
[6] Goovaerts P. Performance comparison of geostatistical algorithms for incorportaing elevation into the mapping of precipitation. GeoComputation, 1999.
[7] Kang S., Kim S., Lee D. Spatial and temporal patterns of solar radiation based on topography and air temperature. Canadian Journal of Forest Research, 32, p. 487-497, 2002.
[8] Krcho J.Morphometric analysis and digital models of georelief. VEDA, Bratislava (in Slovak), 1990.
[9] Matheron G. Principles of geostatistics, Economic Geology, 58, p. 1246-1266, 1963.
[10] Saveliev Anatoly A., Mucharamova Svetlana S., Piliugin Gennady A. Modeling of the daily rainfall Values using surface under tension and Kriging. Journal of Geographic Information and Decision Analysis, 2 (2), p.52-64, 1998.
[11] Šúri M. A new GIS-based solar radiation model and its application to photovoltaic assessments. Transaction in GIS, 8 (2), p. 175-190, 2004.
[12] Venables W.N., Ripley B.D. Modern applied statistics with S-PLUS. New York: Springer, 1999.